Published in final edited form as:
Ultrasound Med Biol. 2011 June ; 37(6): 900–908. doi:10.1016/j.ultrasmedbio.2011.03.011.

Validation of Dynamic Contrast Enhanced Ultrasound in Rodent Kidneys as an Absolute Quantitative Method for Measuring Blood Perfusion

Paul Kogan, BS[1,†], **Kennita A. Johnson, PhD**[1,†], **Steven Feingold, BS**[1], **Nicholas Garrett, BS**[2], **Ismayil Guracar, MS**[3], **William J. Arendshorst, PhD**[2], and **Paul A. Dayton, PhD**[1]

[1]Joint Dept. of Biomedical Engineering, University of North Carolina - North Carolina State University, Chapel Hill, NC, USA

[2]Dept. of Cell and Molecular Physiology, University of North Carolina, Chapel Hill, NC, USA

[3]Siemens Medical Solutions, Mountain View, CA

Abstract

Contrast-enhanced ultrasound (CEUS) has demonstrated utility in the monitoring of blood flow in tissues, organs, and tumors. However, current CEUS methods typically provide only relative image-derived measurements, rather than quantitative values of blood flow in milliliters/minute per gram of tissue. In this study, CEUS derived parameters of blood flow are compared to absolute measurements of blood flow in rodent kidneys. Additionally, the effect of contrast agent infusion rate and transducer orientation on image-derived perfusion measurements are assessed. Both wash-in curve and time-to-refill algorithms are examined. Data illustrate that for all conditions, image-derived flow measurements were well-correlated with transit-time flow probe measurements ($R > 0.9$). However, we report differences in the sensitivity to flow across different transducer orientations as well as the contrast analysis algorithm utilized. Results also indicate that there exists a range of contrast agent flow rates for which image-derived estimates are consistent.

Keywords

destruction-reperfusion; flash replenishment; microbubble; contrast agent; blood flow; perfusion

Introduction

Contrast-enhanced ultrasound imaging (CEUS) has encouraging potential for non-invasive assessment of tissue and organ health as well as the assessment of tumor response to therapy. Research studies to date have demonstrated that individual microbubble contrast agents (MCA) can be detected with a clinical ultrasound system, providing extraordinary sensitivity to blood flow in both large and small vessels (Goldberg 2001, Klibanov et al. 2004; Sboros and Tang 2010). Indeed, the most common application of contrast-enhanced ultrasound imaging is for blood perfusion imaging, and CEUS has demonstrated promise in assessing perfusion and neoplasms of the heart, liver, kidney, spleen, pancreas as well as

Corresponding Author: Paul Dayton, Ph.D. 304 Taylor Hall, CB 7575 Chapel Hill, NC, 27599 Phone: (919) 843 9521 Fax: (919) 843 9520 padayton@bme.unc.edu.
†These authors contributed equally to this work.

Disclosures:
P.A.D. is on the Scientific Advisory Board for Targeson LLC. The Dayton Lab has collaborations with Siemens Medical Solutions, Visulasonics, Inc., and Lantheus Medical Imaging, Inc., although none of these collaborations involve financial exchange.

other organs and tissues (Goldberg 2001; Wilson and Burns, 2010; Cosgrove and Lassau, 2010). CEUS has significant advantages over other imaging modalities such as Magnetic Resonance Imaging (MRI) and computed tomography (CT) due to its portability, low cost, and real-time capability (Gessner and Dayton 2010). Additionally, CEUS may provide one of the only safe and non-invasive methods of imaging perfusion in the presence of renal insufficiency, since contrast enhanced MRI and CT imaging techniques are contraindicated in this population (Huang et al. 2006; Lind Ramskov and Thomsen 2009). These factors are encouraging increased studies for the pre-clinical (Sullivan et al. 2009) and clinical (Kalantarinia 2009; Kalantarinia et al. 2009) application of CEUS in assessment of renal function.

While CEUS imaging techniques can provide relative measurements of tissue perfusion, they have not yet been used for absolute quantitative measurements. We hypothesize that one reason CEUS is used only for relative measurements is that contrast agent administration parameters and transducer orientation may bias measurements, preventing an established calibration between imaging derived measurements and absolute flow.

In the present work, we examine two methods of CEUS perfusion imaging based on the ability of ultrasound to modulate the contrast agent flow into the tissue of interest by clearing the microbubbles using a high-energy (but still within diagnostic limits) acoustic pulse. Both methods use low-intensity (not destructive to contrast agents) ultrasound to observe contrast enter the kidney microvasculature, and then assess flow “rate” by either fitting the wash-in rate to a model (Wei et al. 2001; Klibanov et al. 2004; Strouthos et al. 2010) or by estimating the time for the contrast signal to return to a set percentage of maximum signal enhancement (Chomas et al. 2003; Pollard et al. 2009; Feingold et al. 2010). Our studies extend the pilot study originally performed by Wei et al. (2001), which compared renal tissue perfusion using contrast-enhanced ultrasound with an ultrasonic flow probe in dogs. Since approximately 90% of total RBF supplies the cortex (Young et al. 1996), they used cortical microbubble velocity as a surrogate for total RBF and found an excellent correlation with the ultrasonic flow probe ($R = 0.82$). This early assessment was a promising indication of the absolute quantitative potential of CEUS, however, these studies were not continued or expanded systematically to assess robustness of this technique as a function of imaging parameters.

The kidney serves as a good model for measurements of organ blood flow since it is highly vascular, readily imaged with ultrasound, and typically has a single feeder artery. There are several methods of measuring real-time RBF. Calibrated perivascular transit-time flow probes provide the sensitivity and accuracy needed for detecting rapid changes in RBF in the form of volumetric flow rates (Welch et al. 1995). However, they commonly require fitting around an exposed portion of the renal artery of an anesthetized animal, making this method invasive. In addition, while detecting global changes in RBF they cannot delineate changes in intrarenal perfusion to distinct medullary or cortical areas. Fiberoptic light guides connected to Laser-Doppler flowmeters can provide fast regional perfusion estimates by measuring red blood cell flux. However, their drawbacks include invasive application, uncertainty in placement, limited tissue sampling, and relative perfusion units (Sullivan et al. 2009).

Thus, to work towards the future goal of utilizing CEUS for absolute measurements of tissue blood perfusion, the purpose of the present study is to validate CEUS-derived measurements of renal blood perfusion with absolute values of ml/min per gram of tissue based on a calibrated flow probe. Furthermore, we provide new information about the effects of parameters such as contrast agent administration rate and transducer positioning on two

different image-derived measurements. These data advance our understanding of parameter regimes where CEUS is accurate and reproducible.

Materials and Methods

Animal preparation

All experimental procedures were approved by University of North Carolina Institutional Animal Care and Use Committee. Male Sprague-Dawley rats (350 – 750 g, N = 10) were anesthetized with intraperitoneal injections of sodium pentobarbital (50 mg/kg bwt). The animals were placed on a heated surgical platform and a 24-gauge indwelling tail vein catheter was inserted for intravenous (IV) infusion of bovine serum albumin (4.75% BSA) at 10 μl/min throughout the surgery to maintain blood volume. A catheter was placed in the bladder to facilitate micturition and prevent hydronephrosis throughout the procedure and imaging. A tracheotomy was performed to facilitate free breathing and minimize dead space. The tracheal tube was connected to a 100% oxygen source flowing at 1 L/min. A catheter connected to a pressure transducer was inserted into the right femoral artery to measure mean arterial pressure. A catheter was inserted in the left common iliac artery and fed up the abdominal aorta to the origin of the left renal artery to administer Angiotensin II (Ang II, 20 ng/ul) directly to the kidney. The left kidney was exposed and a transit-time flow probe (TS420 Perivascular Flowmeter, Transonic Systems, Ithaca, NY) was placed on the renal artery to measure renal volumetric blood flow. Because the flow probe measures RBF acoustically, it was not used concurrently with CEUS so as to avoid interference between the two systems. A baseline reading of the volumetric blood flow from the transit-time flow probe was recorded prior to imaging. After the experimental setup was complete, the animal was allowed to stabilize for 1 hour prior to commencing imaging.

Ultrasound Imaging

Ultrasound imaging was performed with an Acuson Sequoia 512 system (Siemens Medical Solutions USA, Inc., Mountain View, CA) using two 15L8 linear array transducers. Ultrasonic gel was applied over the kidney and the ultrasound transducers were fixed with clamps to image the parasagittal and the coronal planes. Acquisition of imaging data was alternated between the two planes so that signal from the two transducers did not interfere with each other. The MCA was a preclinical lipid-shelled perfluorocarbon microbubble prepared in-house (Streeter et al. 2010). MCAs were diluted in saline to get an average concentration of 1.6×10^9 bubbles/mL with a mean diameter of 0.76 (± 0.25) μm. Infusion was through the tail vein catheter via a computer-controlled syringe pump (Harvard Apparatus, Holliston, MA). Care was taken to prepare the contrast solution consistently prior to each experiment in order to achieve the same concentration in the syringe.

For each orientation, renal perfusion was estimated through two methods previously described in the literature. The first method used a motion-stabilized destruction-reperfusion parametric imaging technique based on the time for contrast signal at each pixel to recover to a percent of its original value after contrast clearance (referred to as “the parametric method” in this manuscript). Further details of this technique have been previously described in detail by Pollard et al. (2009). Briefly, this parametric imaging technique involved clearance of the contrast agent using a 1 second higher-energy ultrasound pulse (mechanical index (MI)=1.9), followed by lower-energy (MI=0.18) imaging in Cadence CPS mode at 7 MHz for 20 seconds. Frame-to-frame image data were aligned based on the derived B-mode data and the time-to-20% return of full-scale intensity was calculated for each pixel. The final product was an image with values displayed over the kidney region of interest (ROI) through a time-indexed color map which were analyzed offline. Each measurement was taken twice for averaging during for analysis.

The second imaging method involved assessing the parameters of wash-in curves after contrast clearance, and is referred to in this manuscript as the “wash-in curve method”. This technique has also been thoroughly described in the literature (Wei et al. 1998; Wei et al. 2001; Sullivan et al. 2009). Briefly, contrast refill into the kidney was digitally recorded using low-MI CPS mode after clearance of the contrast agent using the same high-energy ultrasound pulse as described above. Thirty second videos at 15 Hz were recorded using the “Cine” feature on the Sequoia, which were then analyzed off-line. The regional signal intensity in each frame was plotted against time and fitted with a mono-exponential equation which yielded quantitative parameters analogous to microbubble velocity and tissue perfusion.

The two techniques used for calculating tissue perfusion in this study differ in a number of key areas. The parametric method calculates reperfusion times on a pixel-by-pixel basis and later averages these values to determine the overall perfusion rate for a given ROI. The wash-in curve method cumulates data from an ROI first, and then fits the data to a curve to generate perfusion information. The algorithm used to calculate perfusion in the parametric method is a threshold detection for contrast to either be absent or present, while the wash in curve method uses an algorithm to fit an exponential curve to the data. Both methods have been used in the literature for contrast-enhanced blood perfusion measurements. One of our goals was to compare the effectiveness of these two techniques in detecting changes in perfusion rate as well as dealing with variations in contrast agent concentration.

Once data were collected in both the coronal and parasagittal orientations, the MCA infusion rate was increased and the imaging procedures were repeated. When imaging was completed for all the infusion rates, the MCA infusion was stopped. Circulating microbubbles caused substantial noise spikes on the transit-time flow probe. The imaging transducer correlated the presence of circulating bubbles with this noise. The blood stream was considered to be cleared when the transit-time flow probe returned to the baseline value (without noise spikes) prior to the microbubble injection. BSA was infused through the tail vein while the MCA were allowed to clear the blood and a final transit-time flow probe measurement was taken. In order to modulate renal blood flow, an effective Ang II dose ranging from 8 - 320 ng/(kg·min) was infused into the left renal artery to decrease the RBF by 3.5% - 77% The animal was allowed to stabilize for 30 minutes following adjustment in Ang II dose. Imaging was repeated for all orientations and MCA infusion rates, and three RBF rates – a baseline rate, and two reduced flow rates produced after two different doses of Ang II. One aged rat had an extremely low baseline RBF of 0.32 ml/(g·min), possibly due to advanced glomerulosclerosis and did not receive Ang II. A second rat was unresponsive to a second dose of Ang II and was imaged for only two stable RBFs. After imaging, the rats were euthanized with an overdose of anesthetic and the left kidney removed and weighed. All image data was retrieved from the Sequoia at the end of each imaging sessions and exported in DICOM format with JPEG compression.

Data Analysis Methods

RBF measured with the transit-time flow probe was normalized by the kidney weight in order to get the RBF per gram of kidney weight (KW). The MCA infusion rates were also normalized by KW to standardize the infusion rates for data comparison.

For the parametric method, color-map images were manually segmented into cortical, outer, and inner medullary regions of interest (ROI) (Figure 1). When selecting the cortical, inner medullary, and outer medullary regions, multiple observational tactics were employed. Care was taken to note structures such as the arcuate arteries (seen as green lines parallel to the capsule) and vasa recta (red or purple striations perpendicular to the capsule) in order to distinguish the cortex from outer medulla, while differences in echogenicity seen in

corresponding B-mode images distinguished the outer medulla from the inner medulla. Reperfusion time data was generated for each pixel based on the colormap in Matlab (Mathworks, Natick, MA). The reperfusion time for the 2 color-maps per ROI, orientation and infusion rates were averaged. Reperfusion rates (RPR) were determined by taking the inverse of the reperfusion time. The cortex is responsible for 90% of RBF, the outer medulla 8% and the inner medulla 2% (Pallone et al. 1990; Young et al. 1996; Arendshorst and Navar 2007; Navar et al. 2008). To get a RPR for the entire kidney, the RPR from the 3 regions were combined using the following equation:

$$RPR_{Kidney} = 0.9 \cdot RPR_{Cortex} + 0.08 \cdot RPR_{Outer\ medulla} + 0.02 \cdot RPR_{Inner\ Medulla} \quad (1)$$

For all animals, MCA infusion rate/kidney weight (KW), RBF and RPR data were imported into Excel (Microsoft, Redmond, WA). For each orientation, the data was sorted by MCA infusion rate/KW, grouped into N = 20 and the average MCA infusion rate/KW was found for each group. For each MCA infusion rate group, linear regression was performed on RPR vs. RBF for both orientations. The intercept was forced to zero and the slope (± standard error) and Pearson's correlation coefficient (R) were calculated.

For the wash-in method, all video data were retrieved from the ultrasound system at the end of each session. Videos were imported into ImageJ (NIH, Bethesda, MD) and ROIs were manually selected for the cortical, inner, and outer medullary regions in a similar manner as the parametric method, with the added benefit of being able to consider the path of the MCAs as they refilled the tissue. As the interlobular arteries refilled, the MCAs moved towards the capsule before turning downwards to the papilla, demarcating the cortex from outer medulla. ROIs in both the coronal and parasagittal sections were selected such that large blood vessels were excluded as much as possible. A z-axis profile of each region produced an intensity vs. time curve that was imported into Matlab. This curve consisted of 3 regions: a pre-destruction portion representing the steady state contrast intensity, the break sequence, and the wash-in region. The wash-in section of the intensity vs. time curve was fit to the equation:

$$y = A \cdot \left(1 - e^{-\beta t}\right) \quad (2)$$

where A is the microbubble intensity at steady state and β is the microbubble rate (Wei et al. 2001; Kalantarinia et al. 2009). Because the microbubbles have to reach the cortex and travel through the outer medulla before the contrast agent reaches the inner medulla, there is a time-delay between the end of the destruction sequence and when the wash-in region exhibits its characteristic exponential shape. A threshold of 8% of the pre-destruction signal intensity was used to exclude this time delay. This thresholding was applied to every intensity vs. time curve prior to curve fitting. Any baseline signal present after the end of the destructive sequence was also removed. Matlab was also used to find the average microbubble intensity before the MCA break (A_{pre}). β was multiplied by (A/A_{pre}) to normalize the data (Chen et al. 2009). Because each region of the kidney contributes to the total RBF differently (Pallone et al. 1990; Young et al. 1996; Arendshorst and Navar 2007; Navar et al. 2008), in order to calculate β for the entire kidney (β_{Kidney}), we used the following equation:

$$\beta_{Kidney} = 0.9 \cdot \beta_{Cortex} + 0.08 \cdot \beta_{Outer\ Medulla} + 0.02 \cdot \beta_{Inner\ Medulla} \quad (3)$$

The MCA infusion rate/KW, RBF, and β for all animals and orientations were imported into Excel and sorted by MCA infusion rate/KW. The data was grouped into N = 20 and the

average MCA infusion rate/KW was found for each group. For each group, linear regression was performed on β vs. RBF for both orientations. The intercept was forced to zero and the slope (± standard error) and Pearson's correlation coefficient (R) were calculated.

Results

Acquired data provided a comprehensive set of measurements indicating the correlation of image-derived perfusion values from the two different perfusion measurement techniques (parametric imaging method and wash-in curve method) with calibrated renal blood flow measurements from the transit-time flow probe. Image-derived measurements were compared to transit-time flow probe measurements for each orientation (coronal and parasagittal), each MCA infusion rate (7 rates), and each dose of Ang II (3 doses) for each animal (N=10).

Parametric imaging method

The parametric imaging method produced perfusion time values for each pixel which were displayed on the ultrasound system as colormaps, where red indicated slower flow and green indicated faster flow. As anticipated, image-derived perfusion time was observed to increase in both the coronal and parasagittal planes (Figure 2) as the dose of Ang II was increased and renal blood flow decreased. This was illustrated best in the coronal plane (2A-2C), with fewer green (more red) pixels in the perfusion-map in both the cortical and medullary regions.

The RPR is the inverse of the perfusion time. RPRs were determined numerically for each region (cortex, outer, and inner medulla) based on image-derived perfusion times, and combined to get a total RPR (RPR_{Kidney}) using Equation 1. For each average MCA infusion rate, RPR_{Kidney} was plotted against the RBF measured by the transit-time flow probe (Figure 3) for both orientations. The slopes and the Pearson's correlation coefficients were found for each set of conditions using linear regression (Table 1).

Wash-in curve method

An intensity vs. time curve of contrast wash-in was also produced for each orientation, MCA infusion rate, dose of Ang II, and subsection of kidney (Figure 4). The cortical, outer medullary, and inner medullary β were combined using Equations 2 and 3 to calculate β for the entire kidney (β_{Kidney}). The β_{Kidney} values were plotted against the RBF measured with the transit-time flow probe (Figure 5) for each set of conditions. The slopes and the Pearson's correlation coefficients were found for each set of conditions using linear regression (Table 2).

Discussion

Results indicated that CEUS measurements of RBF correlated well with the gold standard measurement of RBF from the transit-time flow probe. This was the case for CEUS determinations using both analysis methods ($R > 0.9$ in all cases). One obvious advantage of the ultrasound measurements is that they are less invasive than the use of the transit-time flow probe on the renal artery. Another substantial benefit of ultrasound is that the transit-time flow probe could only measure an overall whole kidney RBF where CEUS can estimate intrarenal flow in different regions of the kidney. The image resolution using 7 MHz was such that we could differentiate cortex from medulla as well as the outer medulla from the inner medulla in the rat.

Renal function is dependent on the age of the rats. This study intentionally involved a wide range of ages and body weight, so the consistency of the methods could be assessed

independent of rat age/weight. Figures 3 and 5 illustrate that the data is consistent for both young and old rats. A wide range of infusion rates were tested (13.6 – 78.2 μl/(g·min)) specifically to determine if the injection dose, with respect to kidney (or body) weight, affects the outcome. In this study, the MCA infusion rates were divided by the animals' kidney weights, which allowed for the normalization of MCA infusion rate for the wide range of animal body weights studied (350 – 750 g). Kidney weights correlated linearly with body weights (Figure 6). Although, this particular study was invasive, in future noninvasive studies, body weights can be used instead of kidney weights to normalize the MCA infusion rates. Moreover, we performed near-simultaneous acquisition from different orientations of the kidney by using 2 transducers - coronal (Figure 2A-2C) and parasagittal (Figure 2D-2F). The slope of the data as a function of known flow (Figures 4 and 7) defines the relationship between image-derived RPR_{Kidney} or β_{Kidney} with the RBF measured by the transit-time flow probe. The steepness of the slope indicates sensitivity of the imaging method to the blood flow changes. The inconsistency of the slope for varying contrast infusion rates indicates a bias as a function of contrast infusion rate. Ideally, the imaging method should demonstrate a steep slope which remains constant over the range of useful contrast infusion rates, indicating high sensitivity and low bias from the contrast agent administration dose.

Sensitivity to Renal Blood Flow

Our observations indicated that the wash-in method was less sensitive than the parametric method in detecting changes in renal blood flow, as suggested by an average slope of 0.26 ± 0.01 and 0.18 ± 0.02 for the wash in method coronal and parasagittal orientations, respectively, compared to 0.46 ± 0.10 and 0.40 ± 0.07 for the parametric method coronal and parasagittal orientations.

Effect of MCA Infusion Rate on RPR and β

Although the wash-in method was less sensitive overall to changes in renal blood flow, this method was also relatively insensitive to MCA infusion rate. The slope of RPR vs. β remained fairly constant over the range of infusion rates tested. For the coronal orientation, the average slope was 0.26 ± 0.01 over all the contrast infusion rates tested and the average slope was 0.18 ± 0.02 for the parasagittal orientation.

Fitting the exponential model to the wash-in data was affected by a number of factors. As already described, the curves generated in the inner medulla included a time delay as the contrast had to first flow through the cortex and outer medulla before it appeared, creating a generally more S-shaped curve. Since the exponential model used could not be fit to such a curve, we used a simple threshold to remove the time-delay portion of the signal. For consistency, the same threshold was applied to all the wash-in curves generated, including the cortex and outer medulla. Because these curves were quick to rise after the end of the break sequence, only one or two data points were removed by the threshold, and the β calculated values were not significantly affected. For very high in-vivo concentrations of microbubbles, the destructive sequence was unable to fully eliminate all contrast signal from within the ROIs. Undestroyed contrast, as well as noise in the images, left a non-zero value immediately after the end of the break sequence. This baseline value was removed via simple subtraction before the curves were fitted.

The slope of the RPR vs. RBF from the parametric method was more sensitive to MCA infusion rate than the wash-in method. The range of slope values over this study range from 0.28 to 0.57 as a function of contrast infusion, which would make it more challenging to utilize this method in a calibrated fashion unless contrast agent administration rate was controlled. For the coronal orientation at contrast infusion rates of 20.0 – 42.1 μl/(g·min), the average slope was constant at 0.44 ± 0.02. For the parasagittal orientation at contrast

infusion rates of 42.1 – 60.6 μl/(g·min), the average slope was constant at 0.45 ± 0.01 – so within these ranges, this method was both sensitive and consistent. However, the lowest infusion rate tested (13.6 μl/(g·min)) produced a slope of 0.28 for both methods.

Slower contrast infusion rates result in a bias in the duration required for contrast signal intensity to reach the level before the clearance pulse. With high infusion rates, superficial microbubbles obscured the acoustic signal and shadowed deeper microbubbles that appeared later during the capture time. In addition, high infusion rates were observed to disrupt the motion correction algorithm in two phases. Immediately following destruction, the rush of MCAs into the kidney appears as a strong moving signal on B-mode, causing the motion correction to lose its tracking reference. With even higher MCA infusion rates, motion correction errors occur during the later phase where the superficial microbubbles overshadow the deeper ones and thus also appear as a loss of signal in the tracking reference. In each orientation, there is a range of MCA infusion rates for which the slope is constant.

Effect of Transducer Orientation on RPR and β

The kidney is a unique organ in that it has a highly structured and polar orientation. This makes it particularly well suited for vascular imaging. In normal variant kidneys, the arterial blood is supplied by a single artery which diverges in a radial pattern up the renal columns between the medullary lobes to the cortex. At the interface of the cortex and medulla the arcuate arteries send off interlobular arteries into the cortex which then branch into the afferent arterioles to supply the glomeruli. Depending on the location of the glomeruli they originate from, the efferent arterioles have very different patterns and distributions. If they originate from cortical glomeruli they form an undifferentiated capillary plexus that supplies the cortex. However if they originate from juxtamedullary glomeruli they form the vasa recta which course deep down into the medulla and follow the loops of Henle. These straight capillaries consist of descending and ascending portions connected by a tight loop and are responsible for the counter-current exchange of water and electrolytes.

In the coronal plane we observed MCAs traveling in slow and straight paths down and then up the medulla. However, in the parasagittal plane such clear trajectories were more difficult to appreciate. We believe that this trajectory was the path of the MCAs through the vasa recta and that the parasagittal plane is perpendicular to the vasa recta while the coronal plane is parallel. In addition, in the parasagittal plane there was a significantly smaller representation of both the inner and outer medulla, making their differentiation from each other more difficult and perhaps less reliable. However because of the relatively little weight placed on the inner medulla and outer medulla (2% and 8% respectively) minor uncertainties in area selection were not propagated to the final perfusion estimates. In both planes differentiation between cortex and outer medulla were comparable.

The orientation of the vasa recta relative to the ultrasound beam did affect both perfusion estimates RPR and β. Observations indicated that for the coronal plane, the slope was average 12% higher for the parametric method and 32% higher for the wash-in method, indicating that the coronal orientation had a higher sensitivity than the parasagittal plane. Our explanation for this difference is that when the acoustic beam is parallel to the vasculature the bubbles have to traverse a longer path-length in order to refill the entire cleared region, thus increasing the refill time and decreasing the RPR or β. The decreased refill rate also affords the ultrasound system more time to capture the MCA reperfusion, perhaps explaining the accompanying increased sensitivity to changes in RBF in the coronal plane.

Study Limitations

One notable limitation of this study was that measurements were only acquired in one image slice for both methods. Since we used a positioning clamp, we were able to maintain the transducer plane constant within each animal study. However, there was still some variability as to whether we chose the exact center of the kidney for each animal. Choosing a slice that was not in the same plane in each kidney might bias the flow measurements as each plane has its own characteristic path-length profile which affects the refill rate. Due to the visualization of the renal papilla in the coronal plane, we hypothesize that it was easier to position the transducer reproducibly in the center plane of the kidney during coronal imaging. In many small animal imaging studies, the parasagittal plane is used rather than the coronal plane, due to convenience in positioning the transducer on a supine animal. However, we hypothesize that we could reduce error in positioning in either imaging plane by using 3D imaging for the parametric method, as previously described by Feingold et al. (2010).

Conclusion

Choosing the right MCA infusion rate is a balance between having enough contrast agent present to achieve sufficient signal without over-saturating, which results in shadowing or the inability to clear the agent with a destructive pulse. Also, since there are volume limitations on the amount of MCA that can be infused into an animal during an imaging session, flexibility is needed in the MCA infusion rate to accommodate the animal's size. Our studies reveal the effect of contrast agent administration dose and transducer orientation on the accuracy and repeatability of ultrasound-derived absolute blood perfusion measurements. Results indicate that under appropriate conditions, CEUS can be utilized as a calibrated quantitative measurement of perfusion in-vivo with enough sensitivity to evaluate differences in regional responses to vasoactive drugs. This could potentially further enable physicians and scientists who wish to non-invasively study long term effects of hypertension and vasoactive drugs on regional renal microvasculature.

Acknowledgments

We appreciate the consultation of Rachel Cianciolo, DVM, in initial discussions of study planning, and the contributions of James Tsuruta with contrast agent formulation.

Sources of Funding: This work was supported by NIH Research Grant HL-02334 (WJA) and a Pilot Study Grant from the UNC Lineberger Cancer Center (PAD).

Non Standard Abbreviations

ANGII	Angiotensin II
CEUS	Contrast-enhanced Ultrasonography
CT	Computerized Tomography
KW	Kidney weight
MCA	Microbubble Contrast Agents
MRI	Magnetic Resonance Imaging
RBF	Renal Blood Flow
ROI	Region of Interest
RPR	Reperfusion Rate

References

Arendshorst, W.; Navar, L. Renal Circulation and Glomerular Hemodyamics.. In: Schrier, editor. Diseases of the Kidney and Urinary Tract. Lippincott Williams & Wilkins; Philadelphia: 2007.

Chen NG, Fowlkes JB, Carson PL, Schipper MJ, LeCarpentier GL. Rapid 3-D imaging of contrast flow: application in a perfused kidney phantom. Ultrasound Med Biol. 2009; 35:813–28. [PubMed: 19345468]

Chomas JE, Pollard RE, Sadlowski AR, Griffey SM, Wisner ER, Ferrara KW. Contrast-enhanced US of microcirculation of superficially implanted tumors in rats. Radiology. 2003; 229:439–46. [PubMed: 14526091]

Cosgrove D, Lassau N. Imaging of perfusion using ultrasound. Eur J Nucl Med Mol Imaging. 2010; 37(Suppl 1):S65–85. [PubMed: 20640418]

Feingold S, Gessner R, Guracar IM, Dayton PA. Quantitative volumetric perfusion mapping of the microvasculature using contrast ultrasound. Invest Radiol. 2010; 45:669–74. [PubMed: 20808232]

Gessner R, Dayton PA. Advances in molecular imaging with ultrasound. Mol Imaging. 2010; 9:117–27. [PubMed: 20487678]

Goldberg, BB.; Raichlen, JS.; Forsberg, F. Ultrasound Contrast Agents: Basic Principals and Applications. Martin Dunitz; London: 2001.

Huang WC, Levey AS, Serio AM, Snyder M, Vickers AJ, Raj GV, Scardino PT, Russo P. Chronic kidney disease after nephrectomy in patients with renal cortical tumours: a retrospective cohort study. Lancet Oncol. 2006; 7:735–40. [PubMed: 16945768]

Kalantarinia K. Novel imaging techniques in acute kidney injury. Curr Drug Targets. 2009; 10:1184–9. [PubMed: 19715540]

Kalantarinia K, Belcik JT, Patrie JT, Wei K. Real-time measurement of renal blood flow in healthy subjects using contrast-enhanced ultrasound. Am J Physiol Renal Physiol. 2009; 297:F1129–34. [PubMed: 19625375]

Klibanov AL, Rasche PT, Hughes MS, Wojdyla JK, Galen KP, Wible JH Jr. Brandenburger GH. Detection of individual microbubbles of ultrasound contrast agents: imaging of free-floating and targeted bubbles. Invest Radiol. 2004; 39:187–95. [PubMed: 15076011]

Lind Ramskov K, Thomsen HS. Nephrogenic Systemic Fibrosis and Contrast Medium-Induced Nephropathy: A Choice between the Devil and the Deep Blue Sea for Patients with Reduced Renal Function? Acta Radiol. 2009; 50:965–967. [PubMed: 19863403]

Navar, L.; Arendshorst, W.; Pallone, T.; Inscho, E.; Imig, J.; Bell, P. The Renal Microcirculation.. In: Tuma, R.; Duran, W.; Ley, K., editors. APS Handbook of Physiology, Microcirculation. Academic Press (Elsevier); Boston: 2008.

Pallone T, Roberstson C, Jamison R. Renal medullary microcirculation. Physiol Rev. 1990; 70:885–920. [PubMed: 2194225]

Pollard RE, Dayton PA, Watson KD, Hu X, Guracar IM, Ferrara KW. Motion corrected cadence CPS ultrasound for quantifying response to vasoactive drugs in a rat kidney model. Urology. 2009; 74:675–81. [PubMed: 19589583]

Sboros V, Tang MX. The assessment of microvascular flow and tissue perfusion using ultrasound imaging. Proc Inst Mech Eng H. 2010; 224:273–90. [PubMed: 20349819]

Streeter JE, Gessner R, Miles I, Dayton PA. Improving sensitivity in ultrasound molecular imaging by tailoring contrast agent size distribution: in vivo studies. Mol Imaging. 2010; 9:87–95. [PubMed: 20236606]

Strouthos C, Lampaskis M, Sboros V, McNeilly A, Averkiou M. Indicator dilution models for the quantification of microvascular blood flow with bolus administration of ultrasound contrast agents. IEEE Trans Ultrason Ferroelectr Freq Control. 2010; 57:1296–310. [PubMed: 20529706]

Sullivan JC, Wang B, Boesen EI, D'Angelo G, Pollock JS, Pollock DM. Novel use of ultrasound to examine regional blood flow in the mouse kidney. Am J Physiol Renal Physiol. 2009; 297:F228–35. [PubMed: 19420115]

Wei K, Jayaweera AR, Firoozan S, Linka A, Skyba DM, Kaul S. Quantification of myocardial blood flow with ultrasound-induced destruction of microbubbles administered as a constant venous infusion. Circulation. 1998; 97:473–83. [PubMed: 9490243]

Wei K, Le E, Bin JP, Coggins M, Thorpe J, Kaul S. Quantification of renal blood flow with contrast-enhanced ultrasound. J Am Coll Cardiol. 2001; 37:1135–40. [PubMed: 11263620]

Welch WJ, Deng X, Snellen H, Wilcox CS. Validation of miniature ultrasonic transit-time flow probes for measurement of renal blood flow in rats. Am J Physiol. 1995; 268:F175–8. [PubMed: 7840243]

Wilson SR, Burns PN. Microbubble-enhanced US in body imaging: what role? Radiology. 2010; 257(1):24–39. [PubMed: 20851938]

Young LS, Regan MC, Barry MK, Geraghty JG, Fitzpatrick JM. Methods of renal blood flow measurement. Urol Res. 1996; 24:149–60. [PubMed: 8839482]

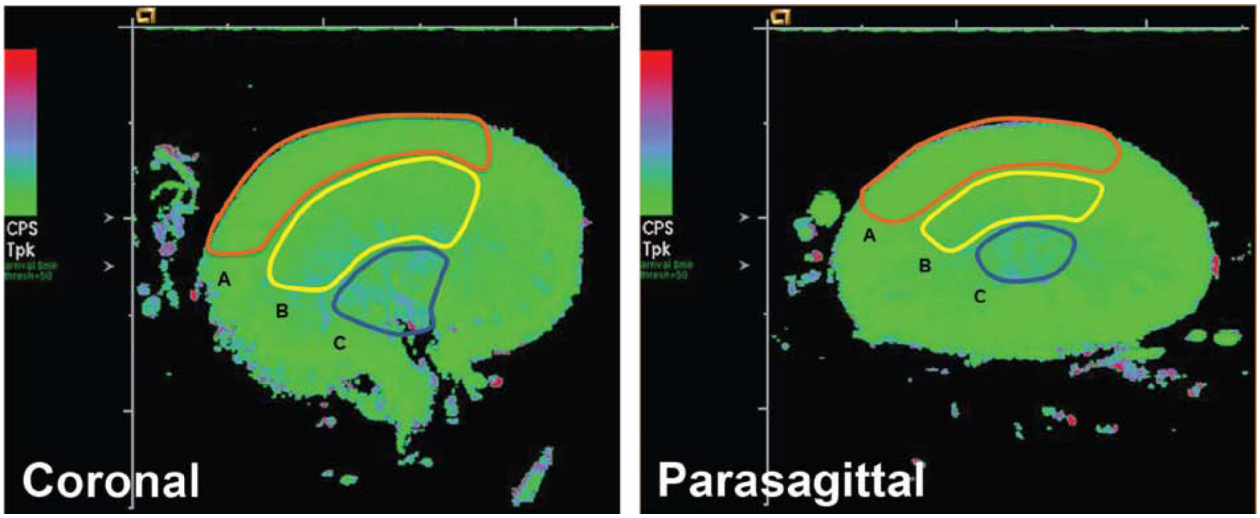

Figure 1.
Representative user selected ROI for a) cortial, b)outer medullary and c) inner medullary regions of the kidney for the coronal (left) and parasagittal (right). The MCA/KW infusion rate for these images was 23.0 μl/g·min.

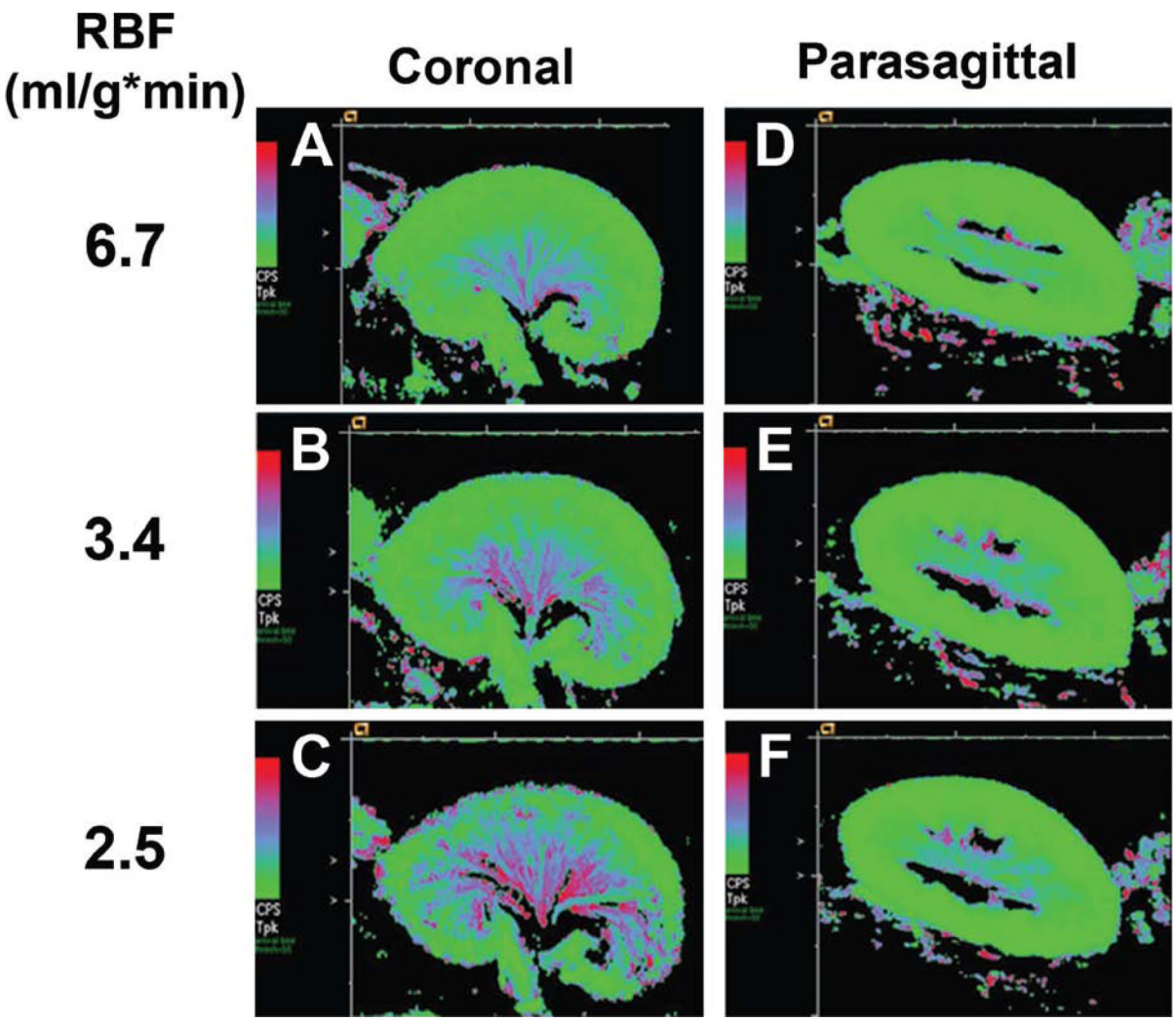

Figure 2.

A representative perfusion map using parametric method for one animal with decreasing renal blood flow (top to bottom). Green indicates faster flow and red indicates slower flow. A-C is the coronal orientation and the D-F is the parasagittal orientation. The MCA/KW infusion rate for these images was 34.0 μl/g·min. In order to reduce the RBF, the animal was given 0, 6 and 10 ng of AngII.

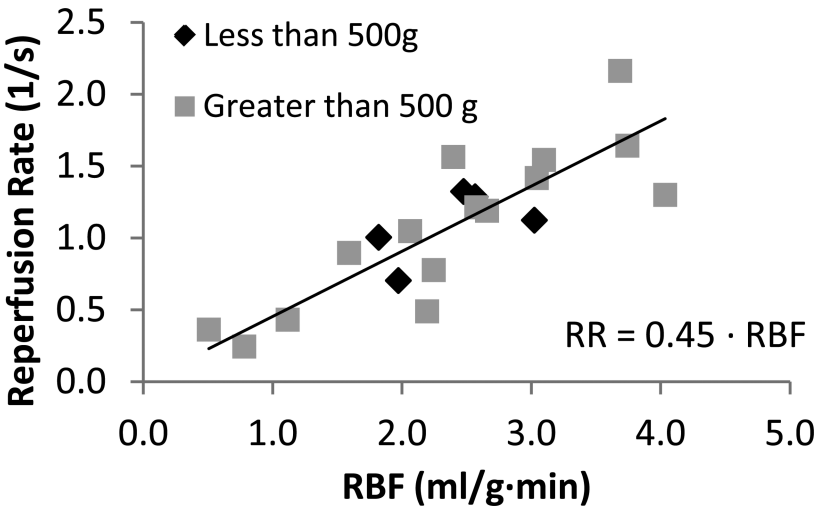

Figure 3.

A representative plot of reperfusion rate (RR) vs. RBF for a single orientation and single MCA infusion rate/KW for both young (■, less than 500g) and old (●, more than 500g) rats.. The MCA/KW infusion rate for this curve is 31.1 μl/g·min in the coronal orientation.

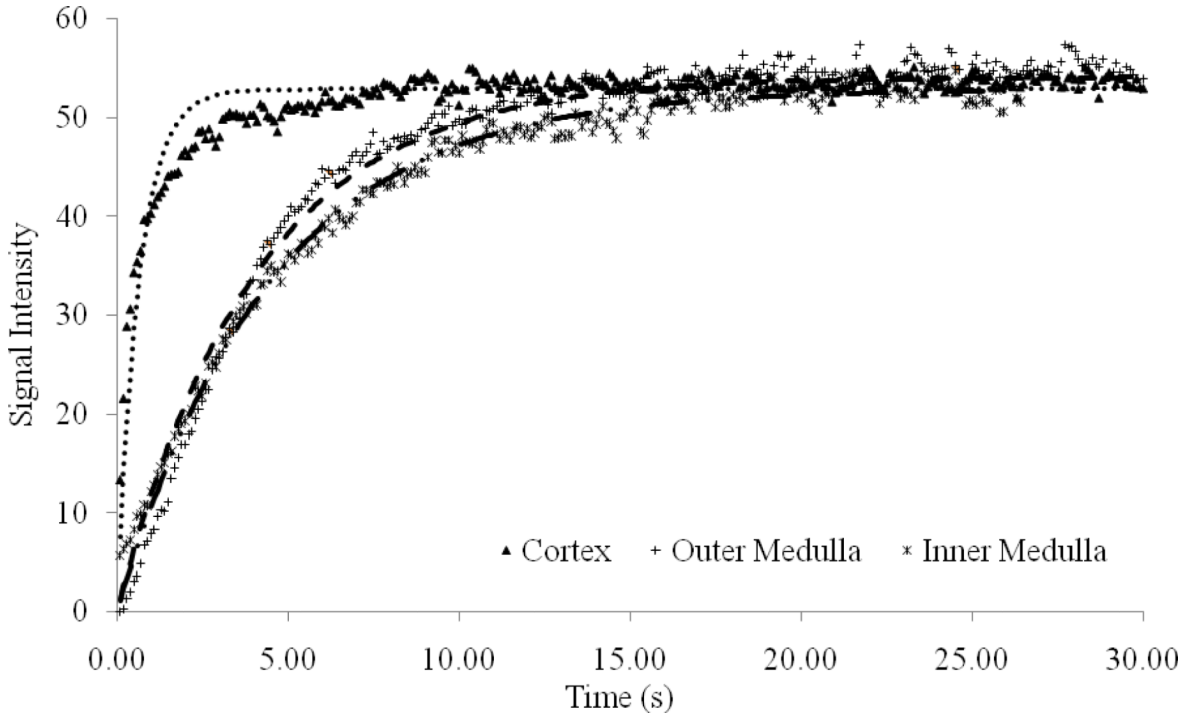

Figure 4.

A representative intensity vs. time curve for the cortical(▲), outer (+) and inner (*) medullary regions of a single kidney. The lines are curve fits to the equation $y = A(1 - e^{-\beta t})$. The MCA/KW infusion rate for this curve is 59.4 μl/g·min in the coronal orientation with 0ng of AngII given to the animal.

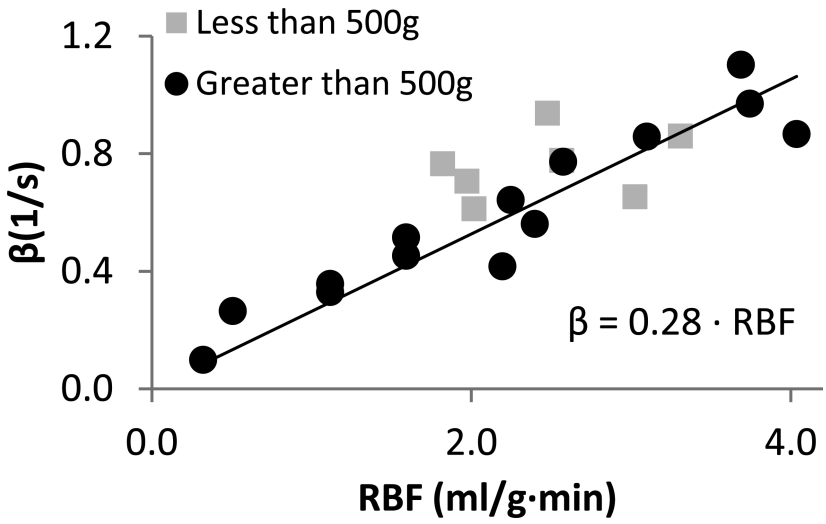

Figure 5.

A representative plot of β vs. RBF for a single orientation and single MCA infusion rate/KW for both young (■, less than 500g) and old (●, more than 500g) rats. The MCA/KW infusion rate for this curve is 52.8 μl/g·min in the coronal orientation.

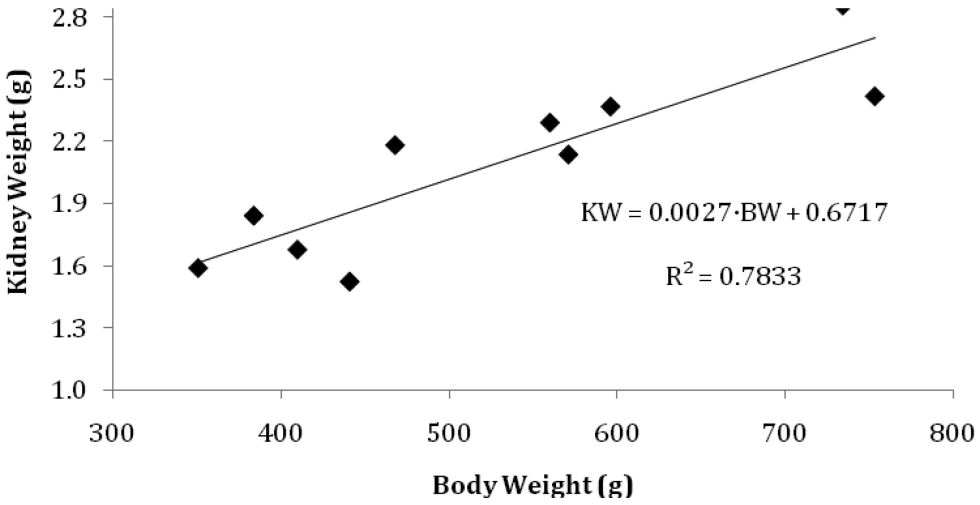

Figure 6.
Kidney weight (KW) vs. body weight (BW) for rats used in this study. Body weights ranged from 350g – 750g. This conversion can be used to convert from body weight to kidney weight in future non-invasive studies.

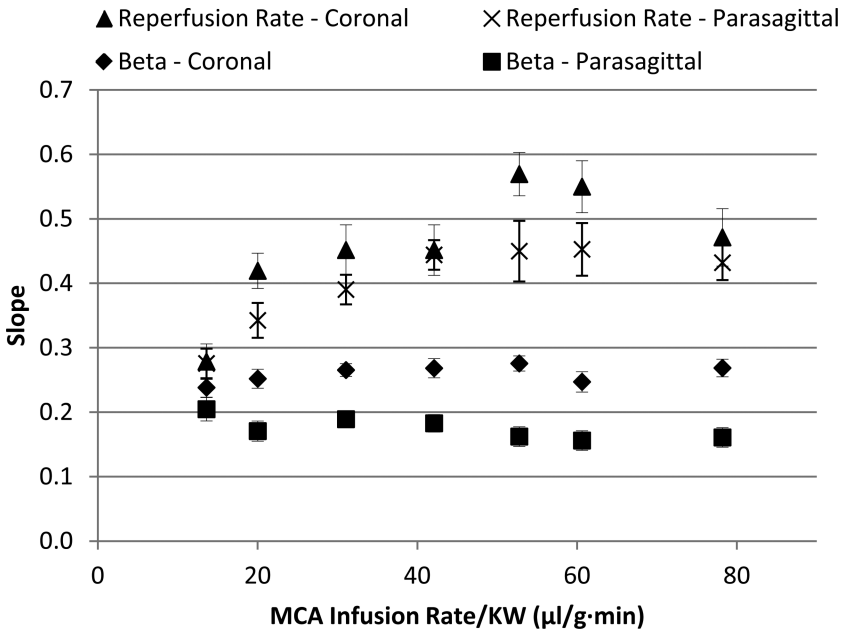

Figure 7.
A plot of the slopes for the RBF vs. either reperfusion rate or β for different mean MCA infusion rates/KW.

Table 1

The slope (± SE) and Pearson's correlation coefficient (R) for the RBF found by the transit-time flow probe vs. the reperfusion rate measured with the perfusion map.

MCA/KW (μl/g*min)	Coronal			Parasagittal		
	Slope	SE	R	Slope	SE	R
13.6	0.28	0.02	0.94	0.28	0.03	0.92
20.0	0.42	0.03	0.96	0.34	0.03	0.94
31.1	0.45	0.02	0.98	0.39	0.04	0.91
42.1	0.45	0.02	0.96	0.44	0.05	0.90
52.8	0.57	0.05	0.94	0.45	0.03	0.95
60.6	0.55	0.04	0.95	0.45	0.04	0.93
78.2	0.47	0.03	0.97	0.43	0.05	0.92

Ultrasound Med Biol. Author manuscript; available in PMC 2012 June 01.

Table 2

The slope (± SE) and Pearson's correlation coefficient (R) for the RBF found by the transit-time flow probe vs. β measured with intensity vs. time curves.

MCA/KW (μl/g*min)	Coronal			Parasagittal		
	Slope	SE	R	Slope	SE	R
13.6	0.24	0.08	0.96	0.21	0.02	0.93
20.0	0.25	0.02	0.97	0.17	0.02	0.93
31.1	0.27	0.01	0.99	0.19	0.01	0.96
42.1	0.27	0.02	0.97	0.18	0.01	0.95
52.8	0.28	0.01	0.98	0.16	0.02	0.92
60.6	0.25	0.02	0.96	0.17	0.02	0.92
78.2	0.27	0.01	0.98	0.16	0.02	0.92